

Feedback from the first stars and galaxies and its influence on structure formation

Benedetta Ciardi

Max Planck Institute for Astrophysics; Karl Schwarzschild Str. 1; 85741 Garching; Germany

Abstract. Once the first sources have formed, their mass deposition, energy injection and emitted radiation can deeply affect the subsequent galaxy formation process and influence the evolution of the IGM via a number of so-called feedback effects. The word 'feedback' is by far one of the most used in modern cosmology, where it is applied to a vast range of situations and astrophysical objects. Generally speaking, the concept of feedback invokes a back reaction of a process on itself or on the causes that have produced it. The character of feedback can be either negative or positive. Here, I will review the present status of investigation of the feedback effects from the first stars and galaxies.

Keywords: First stars; feedback

PACS: <Replace this text with PACS numbers; choose from this list: <http://www.aip..org/pacs/index.html>>

INTRODUCTION

Once the first sources are formed, their mass deposition, energy injection and emitted radiation can deeply affect the subsequent galaxy and star formation process, and the evolution of the intergalactic medium (IGM).

Generally speaking, feedback effects can either reduce (*negative feedback*) or increase (*positive feedback*) the efficiency of the star formation (SF) process. Although a rigorous classification is not feasible because such effects are produced by the same sources and it is hard to separate their individual impact, feedback can be divided into three broad classes (see Ciardi & Ferrara 2005 for a review on the topic): *mechanical*, *chemical* and *radiative*. In addition, reionization and metal enrichment of the IGM could be analyzed as aspects of feedback, but given their relevance and the large amount of literature on these subjects, they will be reviewed elsewhere and here I will concentrate exclusively on mechanical, chemical and radiative feedback.

MECHANICAL FEEDBACK

Mechanical feedback is associated with *mechanical energy injection from winds and/or SN explosions*.

At low redshift mechanical feedback has been extensively studied both in terms of SN explosions and galactic outflows. As strong winds from metal-free or extremely metal poor stars are not expected (although recently few studies demonstrate the contrary; e.g. Meynet, Ekström, Maeder 2006), most of the work at very high redshift has concentrated on the effects of SN explosions (Ferrara 1998; Mac Low & Ferrara 1999; Nishi & Susa 1999; Ciardi et al. 2000; Scannapieco, Ferrara &

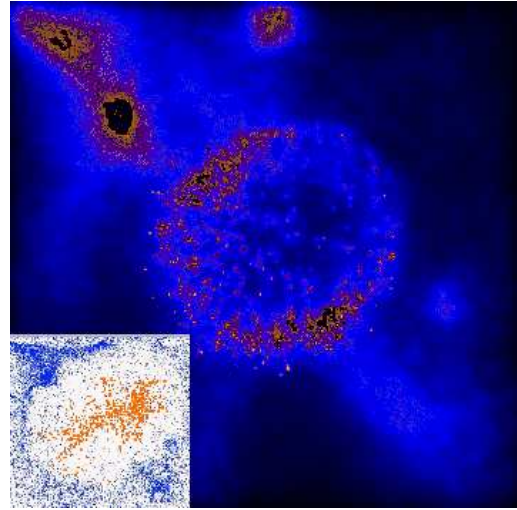


FIGURE 1. Projected gas density $\sim 10^6$ yr after the explosion of a PISN with mass $M_* = 250 M_\odot$ (corresponding to an explosion energy of $E_{\text{SN}} \sim 10^{53}$ ergs) hosted by a halo of mass $M \sim 10^6 M_\odot$ at $z \sim 20$. The box linear physical size is 1 kpc. The SN bubble has expanded to a radius of ~ 200 pc, having evacuated most of the gas in the host halo, that has a virial radius of ~ 150 pc. The dense shell has fragmented into numerous cloudlets. Inset: Metal distribution after 3 Myr. See Bromm, Yoshida & Hernquist (2003) for details.

Broadhurst 2000; Mori, Ferrara & Madau 2002; Bromm, Yoshida & Hernquist 2003; Mackey, Bromm & Hernquist 2003; Wada & Venkatesan 2003; Salvaterra, Ferrara & Schneider 2003; Kitayama & Yoshida 2005; Greif et al. 2007).

A consequence of SN explosions is to expel the gas out of the host halo and reduce the reservoir for subsequent star formation. One of the first studies of such effect

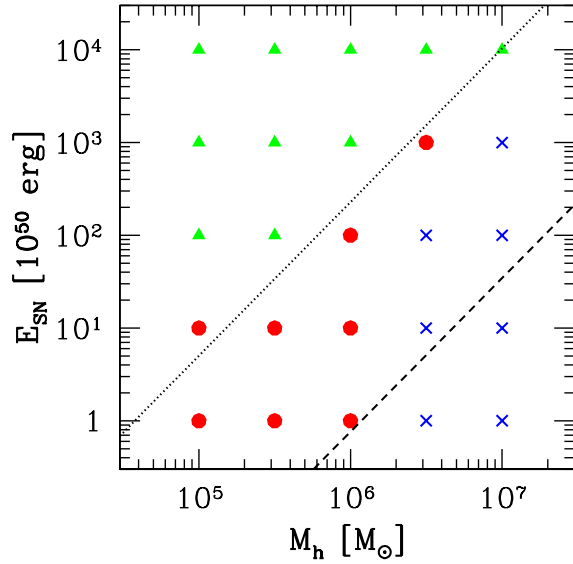


FIGURE 2. Fate of a halo of mass M_h at $z = 20$ hosting a SN explosion with energy E_{SN} . Triangles: more than 90% of the gas is expelled from the halo without pre-existing HII region; circles: more than 90% of the gas is expelled from the halo only with pre-existing HII region; crosses: no substantial gas outflow. Dashed line indicates the halo binding energy (Kitayama & Yoshida 2005).

from Pair Instability SN (PISN) is by Bromm, Yoshida & Hernquist (2003), who run a cosmological SPH simulation until the conditions for the first star formation are met in a halo of mass $M \sim 10^6 M_\odot$ at $z \sim 20$. This configuration is then used as initial conditions to follow the effects of the explosion of such star. The authors assume that the star has either a mass of $M_* = 150 M_\odot$ (corresponding to an explosion energy of $E_{SN} \sim 10^{51}$ ergs) or $M_* = 250 M_\odot$ ($E_{SN} \sim 10^{53}$ ergs). They find that in the former case the host halo remains almost intact, while in the latter it gets completely disrupted (see Fig. 1). A similar result has been reached by Greif et al. (2007), who find that a PISN with $M_* = 200 M_\odot$ ($E_{SN} \sim 10^{52}$ ergs) disrupts the whole host halo.

A parametric study of the effects of varying the explosion energy and the host halo mass is shown in Figure 2, where the fate of the host halo is characterized by different symbols. The results have been obtained using a 3D simulation of the formation of HII regions around the first stars as initial conditions for 1D simulations to follow the effect of SN explosions (Kitayama & Yoshida 2005). In general, the authors find that also if the SN energy is larger than the halo binding energy the gas can still be retained, and that the final fate of the halo strongly depends on the initial conditions, e.g. the existence and extent of a pre-existing HII region produced

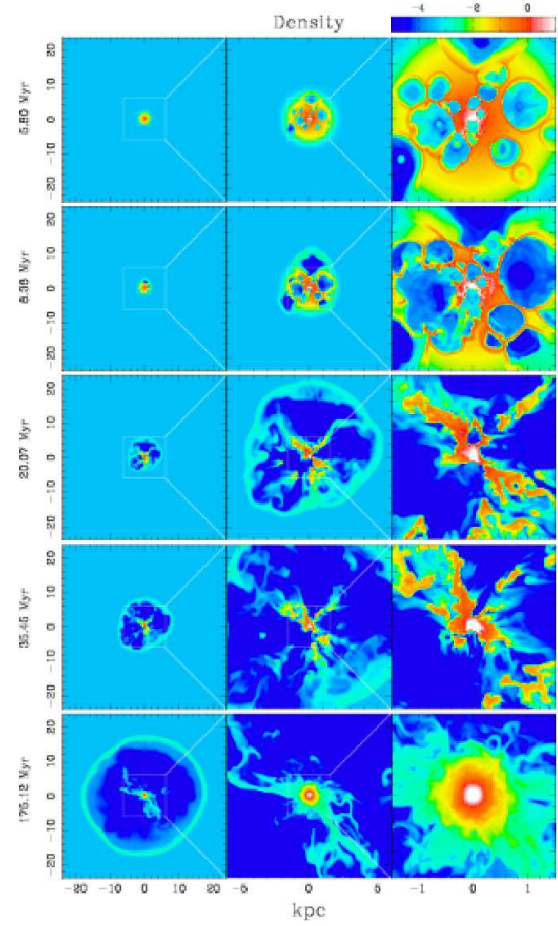


FIGURE 3. Snapshots of the logarithmic number density of the gas in a halo with $M = 10^8 M_\odot$ at $z = 9$, at five different elapsed times (from the top 5.80, 8.36, 20.07, 35.45 and 175.12 Myr) after multiple SNa explosions. The three panels in each row show the spatial density distribution in the $X-Y$ plane on the nested grids (see Mori, Ferrara & Madau 2002 for details).

by the SN precursor. Their results are consistent with the studies mentioned above, as the complete destruction of a halo with mass $M \sim 10^6 M_\odot$ follows an explosion with $E_{SN} \sim 10^{53}$ ergs, while the halo remains intact for $E_{SN} \sim 10^{51}$ ergs.

The situation is more complicated if instead of a single SN, multiple explosions take place. Although such a case has been simulated only for a halo with $M = 10^8 M_\odot$ at lower redshift ($z = 9$; Mori, Ferrara & Madau 2002), this is a good example of what can be expected at higher z . When multiple SNa take place, off-center explosions drive inward propagating shocks that push the gas to the center where a second episode of SF can take place (see Fig. 3). In this case the situation can be very complex and a positive, rather than negative, feedback can be the

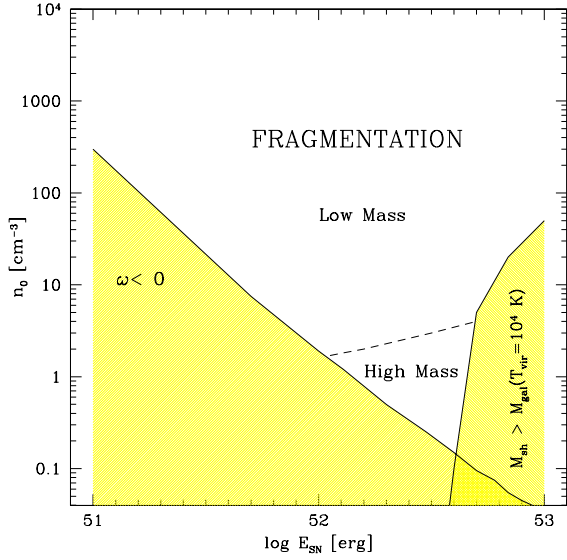


FIGURE 4. Region of the parameter space $E_{\text{SN}}-n_0$ where fragmentation into low-mass ($\sim 1 M_\odot$) or high-mass ($\sim 100 M_\odot$) clumps can occur. Here n_0 is the gas density. Shaded regions are excluded from fragmentation, either because the shell is not gravitationally unstable ($w < 0$) or because the shell mass at the time of instability exceeds the total gas mass of the host galaxy (see Salvaterra, Ferrara & Schneider 2004 for details).

outcome.

In addition to this, other positive feedback effects can follow from the propagation of the shocks, which, sweeping the gas, induce the formation of a dense shell that could eventually fragment and form stars (Mackey, Bromm & Hernquist 2003; Salvaterra, Ferrara & Schneider 2004). Following earlier studies in local environment, Salvaterra, Ferrara & Schneider (2004) derived the conditions expected for such fragmentation to occur (see Fig. 4). Depending on the density of the gas and the explosion energy, low-mass ($\sim 1 M_\odot$) or high-mass ($\sim 100 M_\odot$) clumps, and eventually stars, can form.

In shocked gas (and in general in a partially ionized medium) HD formation is very efficient. As HD cooling lowers the temperature of the gas to values below those reached by molecular hydrogen cooling, the presence of HD in shocks can facilitate fragmentation (Vasiliev & Shchekinov 2005; Johnson & Bromm 2006; Greif et al. 2007). In Figure 5 the HD fraction formed in shocks (solid line) as a function of the Hubble time is shown, compared to the fraction formed through other mechanisms. It is clear that this is by far the most efficient process in producing HD and that its abundance is enough to cool primordial gas down to the cosmic microwave background (CMB) temperature within a Hubble time (bold dashed line).

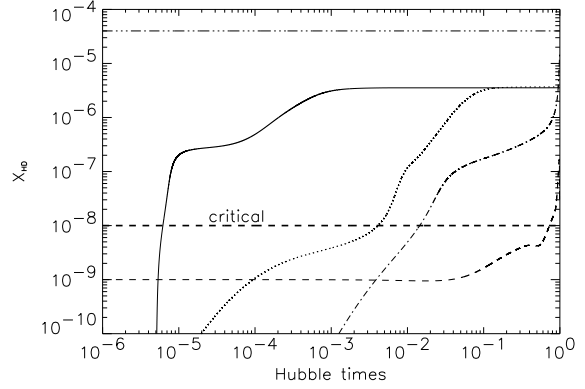


FIGURE 5. Evolution of the abundance of HD, X_{HD} , in primordial gas which cools in four distinct situations. The solid line corresponds to gas compressed and heated by a supernova shock at $z = 20$. The dotted line corresponds to gas shocked in the formation of a 3σ fluctuation dark matter halo at $z = 15$. The dashed line corresponds to unshocked, un-ionized primordial gas collapsing inside a mini-halo at $z = 20$. Finally, the dash-dotted line shows the fraction of HD in primordial gas collapsing inside a relic H II region at $z = 20$. The horizontal line at the top denotes the cosmic abundance of deuterium. The critical abundance of HD denoted by the bold dashed line, is that above which primordial gas can cool to the CMB temperature within a Hubble time. For details see Johnson & Bromm (2006).

To summarize, the above studies suggest that shocks following SN explosions can induce SF and that these stars are typically smaller than those formed in standard conditions, possibly explaining the existence of low-metallicity, low-mass stars. In order to confirm these suggestions 3D studies are required.

CHEMICAL FEEDBACK

Chemical feedback is associated with the existence of a critical metallicity of the gas, Z_{crit} , that induces a transition from a massive to a more standard star formation mode. After the early work of Yoshii & Sabano (1980), chemical feedback has only recently been extensively studied by an increasing number of authors (Bromm et al. 2001; Schneider et al. 2002; Bromm & Loeb 2003; Omukai et al. 2005; Santoro & Shull 2006; Schneider et al. 2006; Tsuribe & Omukai 2006; Clark, Glover & Klessen 2007; Smith & Sigurdsson 2007).

The fragmentation of gas clouds at various metallicities has been investigated following different methods: using 1D (Schneider et al. 2002; Bromm & Loeb 2003; Omukai et al. 2005; Santoro & Shull 2006; Schneider et al. 2006) or 3D (Bromm et al. 2001; Tsuribe & Omukai 2006; Clark, Glover & Klessen 2007) approaches; start-

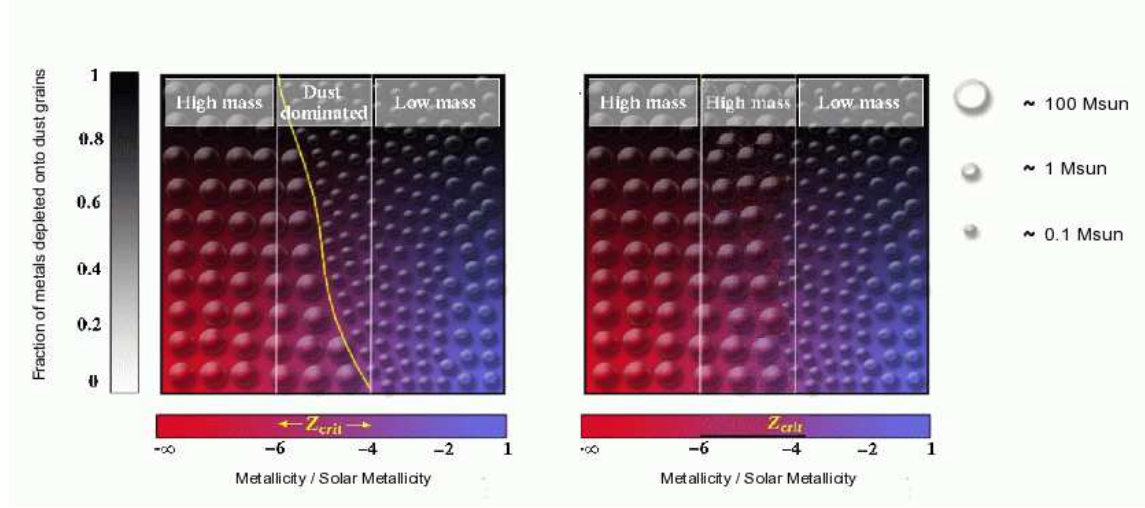


FIGURE 6. Typical mass of clumps that form from the fragmentation of a gas cloud with different metallicity and fraction of metals depleted onto dust grains. The case in which dust is (is not) included is shown in the left (right) panel (original figure in the presence of dust is courtesy of R. Schneider).

ing from cosmological initial conditions or focusing on the collapse of single clouds; including (Clark, Glover & Klessen 2007) or not rotation of the clouds; etc etc. In the early works, only H and He chemistry was followed together with metals of varying global metallicity (Bromm et al. 2001); then the contribution of H_2 and of single metal lines (the most important being CII, OI, SiII and FeII) has been included, and finally also D and dust. What seems to induce the largest scatter in the results of different investigations is the presence of dust. In fact, studies that include dust (Schneider et al. 2002; Omukai et al. 2005; Schneider et al. 2006; Tsuribe & Omukai 2006; Clark, Glover & Klessen 2007) find that clouds with $Z \lesssim 10^{-6} Z_\odot$ typically fragment into clumps of mass $\sim 100 M_\odot$, out of which massive stars can collapse, while if $Z \gtrsim 10^{-4} Z_\odot$ more typical stars form. In the intermediate range $Z = 10^{-6} - 10^{-4} Z_\odot$, the size of the fragment depends on the amount of metals depleted onto dust grains (left panel of Fig. 6). On the other hand, in studies where dust is not included (Bromm et al. 2001; Bromm & Loeb 2003; Santoro & Shull 2006; Smith & Sigurdsson 2007) the formation of high mass stars is prolonged at least to $Z \sim 10^{-4} Z_\odot$ (right panel of Fig. 6). This is exemplified in Figure 6 where the typical clump mass is shown as a function of the original cloud metallicity and the fraction of metals depleted onto dust grains. It seems thus *crucial to clarify the role and characteristics of dust in the early universe*.

In addition to studying the fragmentation properties of gas clouds with different metallicities, *in order to understand chemical feedback, two additional ingredients are required: the initial mass function (IMF) of the first stars and the efficiency of metal enrichment*. In fact, only stars

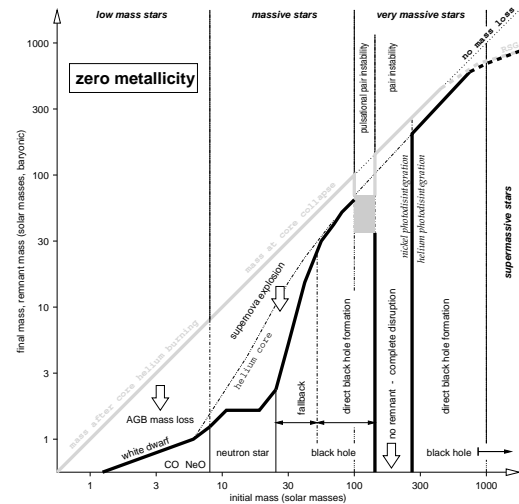


FIGURE 7. Initial-final mass function of non-rotating metal-free stars. The x-axis gives the initial stellar mass. The y-axis gives both the final mass of the collapsed remnant (thick black curve) and the mass of the star when the event begins that produces that remnant (e.g., mass loss in AGB stars, supernova explosion for those stars that make a neutron star, etc.; thick gray curve). See Heger & Woosley (2002) for more details.

in the mass range of SN or PISN explosions contribute to the pollution of IGM (see Fig. 7; although, as mentioned in the previous Section, it seems that also metal-free or extremely metal-poor stars can produce winds and enrich the surrounding medium), and metal enrichment is far from being homogeneous also at low redshift, as is both shown in numerical simulations and observations (see e.g. Fig. 8).

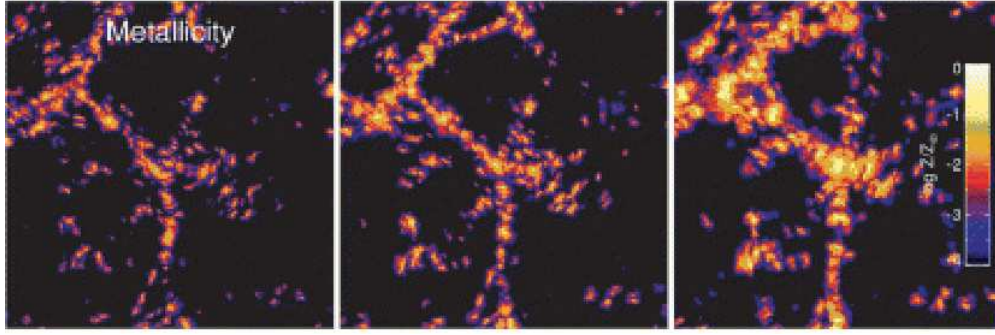


FIGURE 8. A 100 km s^{-1} slice showing the gas metallicity at $z = 4.5, 3.0$, and 1.5 , in a numerical simulation of metal enrichment by Oppenheimer & Davé (2006).

This suggests that the transition from a primordial massive star formation mode towards a more standard star formation mode, which is highly dependent on the local conditions of the gas, takes place at different time in different regions of the universe, and thus that the chemical feedback is a local process.

RADIATIVE FEEDBACK

Radiative feedback is associated with *ionization/dissociation of atoms/molecules and heating of the gas*. The literature on this topic is extremely large (Haiman, Rees & Loeb 1997; Ciardi, Ferrara & Abel 2000; Ciardi et al. 2000; Haiman, Abel & Rees 2000; Susa & Kitayama 2000; Kitayama et al. 2000, 2001; Haiman, Abel & Madau 2001; Machacek, Bryan & Abel 2001; Ricotti, Gnedin & Shull 2002; Yoshida et al. 2003; Dijkstra et al. 2004; Shapiro, Iliev & Raga 2004; Susa & Umemura 2004; Alvarez, Bromm & Shapiro 2006; Ahn & Shapiro 2007; Ciardi & Salvaterra 2007; Johnson, Greif & Bromm 2007) and an exhaustive summary is a difficult task to achieve.

The basic concept is that the minimum mass of objects that collapse in the absence of feedback is $M \sim 10^5 M_\odot$. In the presence of a UV flux instead, objects of such small mass can still form, but their collapse and the amount of cold gas available for SF depends on the strength of the feedback. It should be noticed that, while in the early evolutionary stage the radiation from nearby objects dominates over the background radiation, later on the situation is inverted (Ciardi et al. 2000). It has been shown that the intensity and the sign of this feedback depends on a variety of quantities, like the shape and intensity of the flux. In Figure 9 there is a very simple but illustrative example that shows the effect of a point source with a soft/hard spectrum of different intensity on a uniform medium at different distances from the source. It can be seen that, depending on the characteristics of the

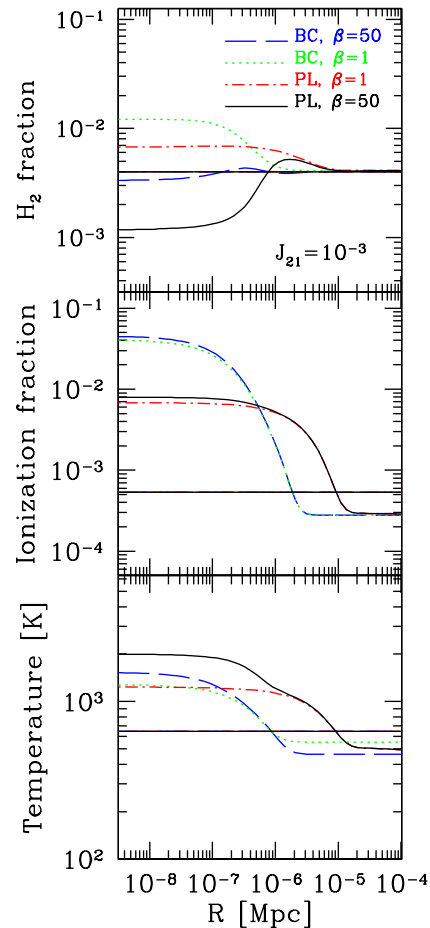


FIGURE 9. Effect of a point source with a soft (BC) or a hard (PL) spectrum of different intensity on a uniform medium at different distances from the source. Molecular hydrogen fraction (top panel), ionization fraction (middle panel) and temperature (lower panel) are shown (see Ciardi et al. (2000) for details).

spectrum and the distance from the source, either positive or negative feedback on molecular hydrogen can be obtained because the main channel for the formation of H_2 is via H^- , and thus the relative abundance of H and electrons is crucial. The situation gets much more complicated in more realistic cases, which will be discussed in the following.

Once the first generation of stars has formed in an object, it can affect the subsequent star formation process by dissociating H_2 in nearby star forming clouds. This is a local, internal feedback. Studies by Omukai & Nishi (1999) and Nishi & Tashiro (2000) show that one massive star produces enough radiation to dissociate the entire host halo. But, if the density distribution of the host halo and its geometry are taken into account, *SF can proceed unimpeded if the star forming clouds are dense and far enough from the star that emits the radiation* (Glover & Brand 2001; Susa & Umemura 2006). As an illustrative example, in Figure 10 the distance at which the dissociating time equals the free-fall time is shown as a function of the cloud number density for different combinations of the H_2 abundance and the mass of the host halo (see Glover & Brand 2001 for details). To put the numbers into perspective, the virial radius of a halo with $M = 10^6$ (10^5) M_\odot at $z = 30$ is about 100 (50) pc. The result is consistent with a 3D hydro simulation with radiative transfer by Susa & Umemura (2006), who study the effect of a star with mass $M_* = 120 M_\odot$, finding that clouds further than 30 pc survive the feedback effect and continue forming stars. This happens not only because of the absorption and geometrical dilution of the radiation, but also because the shell of H_2 forming in front of the I-front traps the dissociating radiation and shields the cloud.

In addition to internal feedback, the radiation emitted by the first stars can affect the IGM and nearby objects evolution. For this reason, it is important to determine how much of the radiation emitted can escape in the IGM, i.e. the escape fraction f_{esc} . Although the situation at low redshift is quite complex and still controversial (i.e. Dove & Shull 1994; Ciardi, Bianchi & Ferrara 2002; Clarke & Oey 2002; Fujita et al. 2003), it seems that there is a consensus on the amount of radiation escaping from massive stars in the early universe, with f_{esc} being larger than 70% and increasing with the mass of the star (Whalen, Abel & Norman 2004; Alvarez, Bromm & Shapiro 2006; Abel, Wise & Bryan 2007; Yoshida et al. 2007; but see also Ricotti & Shull 2000; Wood & Loeb 2000), as can be seen in Figure 11.

One of the first attempts to model self-consistently several feedback effects is a work by Ciardi et al. (2000), in which the authors, among others, study, by means of radiative transfer calculations, the ability of a halo to self-shield against an external soft-UV radiation and to collapse. Figure 12 shows the minimum mass for

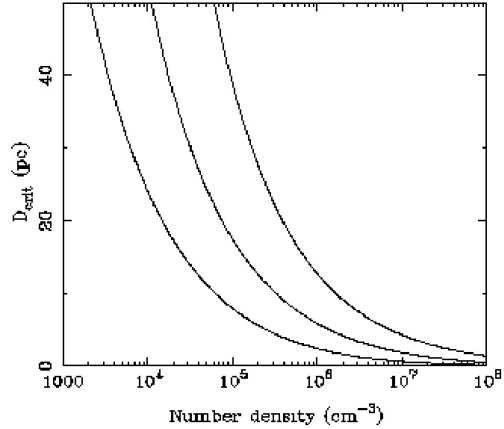


FIGURE 10. Distance at which the dissociating time equals the free-fall time as a function of the cloud number density for different combinations of the H_2 abundance and the mass of the host halo (see Glover & Brand 2001 for details).

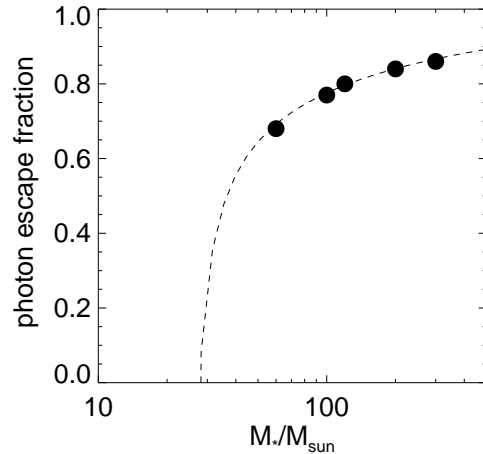


FIGURE 11. Photon escape fraction as a function of the star mass (Yoshida et al. 2007).

self-shielding from an external radiation with varying intensity at the Lyman limit. Calculations are done for different redshifts. The area affected by the feedback is indicated with solid lines. Subsequent investigations tried to improve the modeling by, e.g., including a proper treatment of the hydro.

The Japanese group of Umemura, Susa, Kitayama and collaborators has performed several studies of the collapse of a single halo in the presence of a UV background with radiation hydro simulations, both in 1D and in 3D. In Figure 13 a typical example is shown at $z \sim 10$

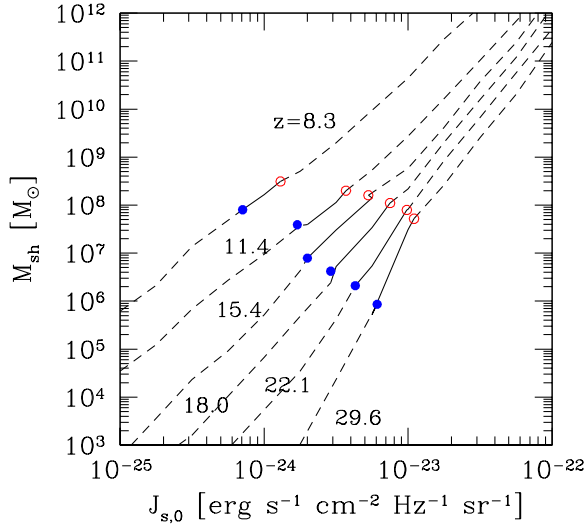


FIGURE 12. Minimum mass for self-shielding from an external radiation with varying intensity at the Lyman limit. Calculations are done for different redshift. The area affected by the feedback is indicated with solid lines. Objects with mass larger than that indicated with open circles can cool via H line cooling, while filled circles indicate the minimum mass for the collapse in the absence of feedback (Ciardi et al. 2000).

for objects with different virial temperature and incident flux. The results for a stellar type source with full radiative transfer treatment are summarized in the lower right panel and show that if $J_{21} < 0.1$ ¹ all objects collapse and cool, while if the mass of the object is $M \gtrsim 10^8 M_\odot$ collapse and cooling happen independently from the value of J_{21} . Otherwise, their fate depends on J_{21} , M and the shape of the spectrum.

A different approach is adopted by a series of studies that, instead of following the collapse of a single object from different initial conditions, run cosmological simulations and analyze the fate of the forming halos. For example, Machacek, Bryan & Abel (2001) find that the collapse and cooling of small mass halos is delayed by the presence of a background, and that the amount of cold gas found in the halos primarily depends on the value of J_{21} and M , as can be seen from Figure 14, in which the fraction of cold gas available for SF in halos in the redshift range $20 < z < 30$ is shown as a function of the mass of the halos and the background radiation. This suggests that objects with mass of a few $10^5 M_\odot$ can retain cold gas and form stars if $J_{21} < 0.1$.

A similar trend (i.e. collapse and cooling are delayed

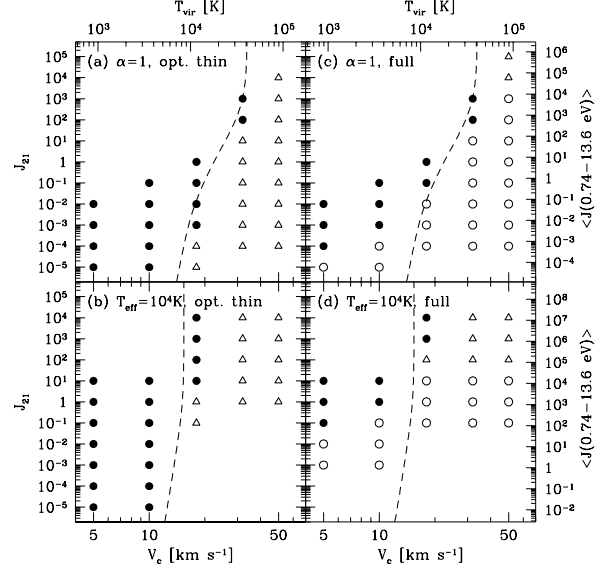


FIGURE 13. Fate of an object forming in a UV background of varying intensity as a function of its virial temperature or circular velocity. Full circles: no collapse takes place; open circles: collapse and cooling take place; open triangles: collapse takes place. Different panels refer to different shape of the incident radiation and optically thin (left panels) or full radiative transfer (right panels) treatment (see Kitayama et al. 2001 for details).

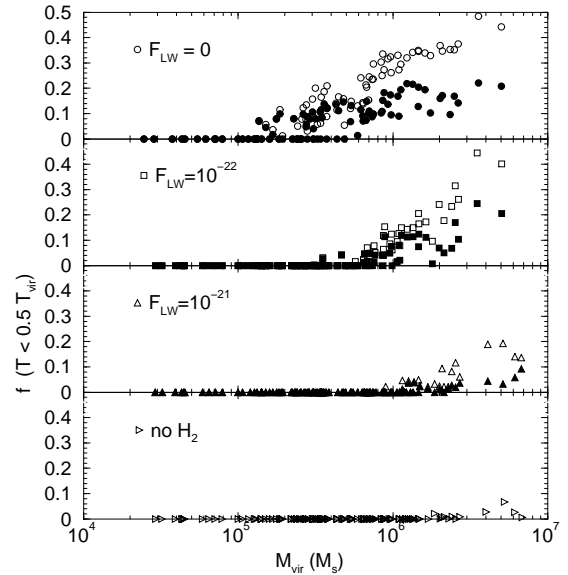


FIGURE 14. Fraction of cold gas within the virial radius as functions of halo mass and soft-UV background flux, F_{LW} . Open symbols represent the fraction of gas that has cooled via H_2 cooling. Filled symbols represent the fraction of cold, dense gas available for star formation (see Machacek, Bryan & Abel 2001 for details).

¹ $J_{21} = 10^{-21} \text{ erg s}^{-1} \text{ cm}^{-2} \text{ Hz}^{-1} \text{ sr}^{-1}$

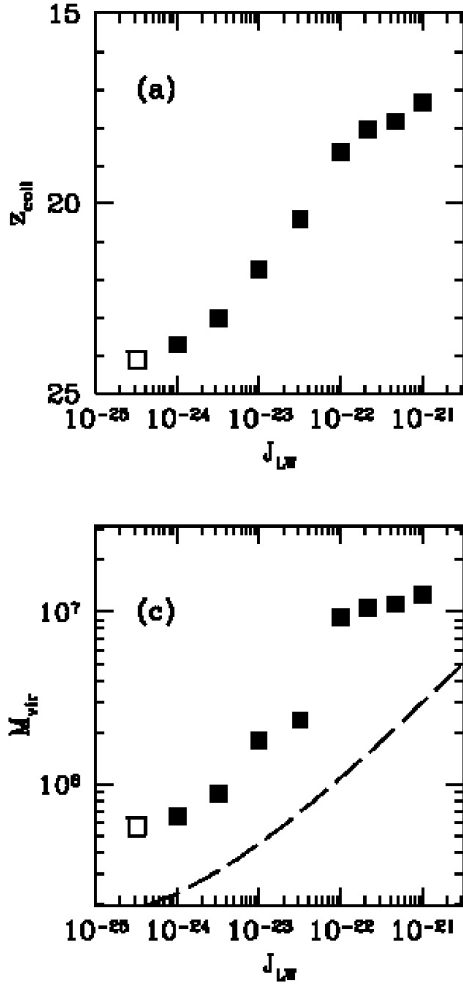


FIGURE 15. Mean halo quantities for several simulations with the same cosmic realization but a range of Lyman-Werner molecular hydrogen photodissociating flux backgrounds (O’Shea & Norman 2007). Upper panel: J_{LW} vs. halo collapse redshift. Lower panel: halo virial mass vs. J_{LW} . The $J_{21} = 0$ “control” results are shown as an open square (it is at $\log J_{\text{LW}} = -24.5$ in the panels which are a function of J_{LW}). In the bottom panel, the dashed line corresponds to the fitting function for threshold mass by Machacek, Bryan & Abel (2001).

by the presence of a background) is found also in O’Shea & Norman (2007). Because of the delay, at the time of the collapse the objects have actually acquired a larger mass. So, for example, an object that would collapse at $z = 24$ with a mass of $M = 5 \times 10^5 M_{\odot}$, in the presence of a background with $J_{21} = 0.1$ would collapse at $z \sim 18$ with a mass $M \sim 10^7 M_{\odot}$ (Fig. 15). This suggests that objects with mass $M < 10^6 M_{\odot}$ are not expected in the presence of a background larger than $J_{21} > 0.01$.

Another different approach to the problem is the one

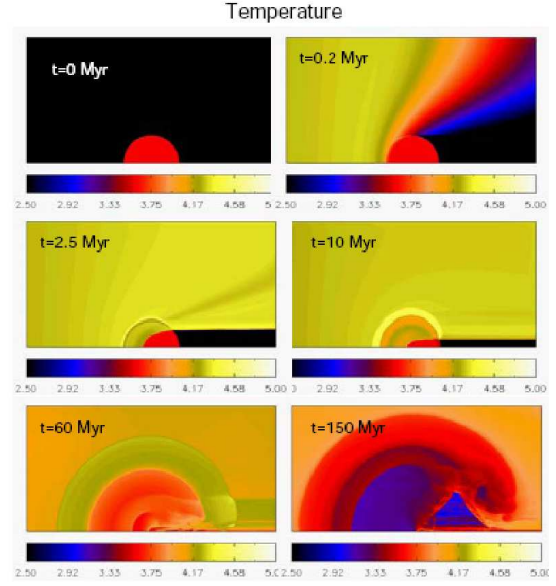


FIGURE 16. Temperature evolution of a mini-halo hit by a photoevaporating flux. Different panel refer to different times (see Shapiro, Iliev & Raga 2004 for details).

by Ahn & Shapiro (2007). The authors use a 1D hydro code with radiative transfer to study the effect of the radiation emitted by a star with mass $M = 120 M_{\odot}$ on the formation of halos of different mass positioned at different distances from the star. Although the results are very sensitive to the initial conditions (including the stage in the halo evolution), objects with $M > 10^5 M_{\odot}$ can generally cool and collapse also if $J_{21} > 0.1$ because the I-front gets trapped before reaching the core of the halos and the shock that develops in front of it leads to positive feedback. The results somewhat contravert other studies, but they might be affected by the 1D configuration which produces unphysical geometric effects. To summarize the effect of dissociating radiation on primordial structure formation *the presence of a UV flux delays the collapse and cooling of small mass halos and the amount of cold gas available primarily depends on the intensity of the flux and the mass of the halo. Some controversy though still exists on the efficiency of such feedback.*

The radiation emitted by the first objects can also photoevaporate small mass halos. This effect has been extensively studied e.g. by Shapiro and collaborators. In Figure 16 a typical example of their simulations shows the temperature evolution of a mini-halo hit by a photoevaporating flux. The time scale for complete photoevaporation though is generally longer than the lifetime of a PopIII star; thus, *in a cosmological context, it is found that mini-halos can generally survive photoevaporation* (Alvarez, Bromm & Shapiro 2006; Abel, Wise & Bryan 2007; but see also Yoshida et al. 2007).

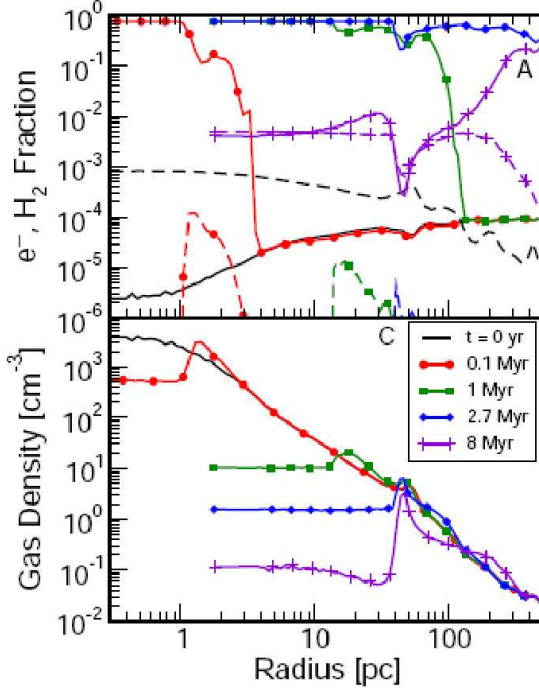


FIGURE 17. Mass weighted radial profiles around the position of a star with mass $M_* = 100 M_\odot$. Upper panel: electron number fraction (solid) and H_2 mass fraction (dashed) for 5 different times, 0, 0.1, 1, 2.7, and 8 Myr after the star is born. The star dies at 2.7 Myr. Lower panel: density evolution (Abel, Wise & Bryan 2007).

In addition to the above negative feedback effects, the radiation produced by the first stars can also favor structure formation, because molecules can efficiently reform, e.g. inside relic HII regions, and induce a positive feedback (Ricotti, Gnedin & Shull 2001; Nagakura & Omukai 2005; O’Shea et al. 2005; Mashchenko, Couchman & Sills 2006; Abel, Wise & Bryan 2007; Johnson, Greif & Bromm 2007; Yoshida et al. 2007). The effect of such positive feedback (that has been first studied by Ricotti and collaborators) can be seen in Figure 17, which shows the abundance of molecular hydrogen and electrons in the vicinity of a source of mass $M_* = 100 M_\odot$ at different times. Although initially H_2 is depleted, eventually, once the star has died (in this case after 2.7 Myr), it efficiently reforms and is available for a new episode of structure/star formation.

In addition to molecular hydrogen, also HD can be efficiently formed inside relic HII regions, with the consequence of reducing further the gas temperature (Nagakura & Omukai 2005; Johnson & Bromm 2006; Yoshida et al. 2007; Yoshida, Omukai & Hernquist 2007). For this reason, it has been proposed that star for-

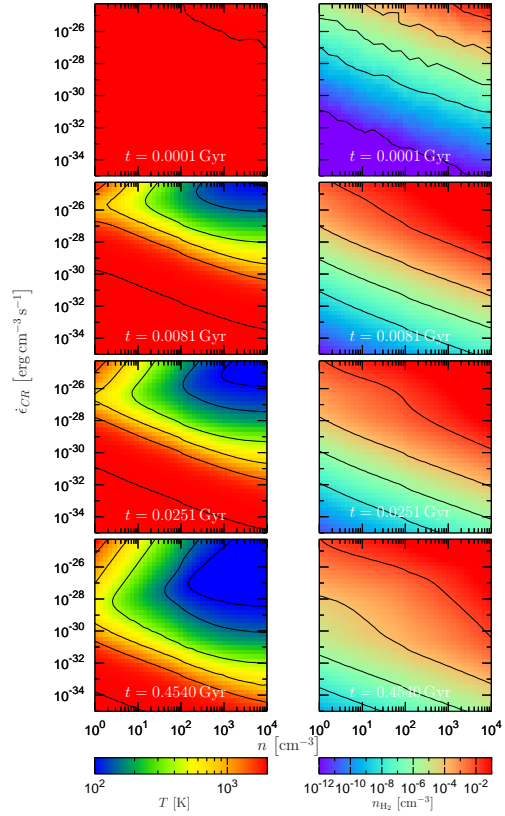


FIGURE 18. Time evolution of the gas temperature (left panels) and the molecular hydrogen abundance (right panels) as a function of the density of the gas, n , and of the cosmic rays injection rate, $\dot{\epsilon}_{CR}$. The gas is embedded in a dissociating flux with $J_{LW} = 10^{-21} \text{ erg cm}^{-2} \text{ Hz}^{-1} \text{ s}^{-1}$. The superimposed contour plots join points of same temperature or same H_2 number density. See Jasche, Ciardi & Ensslin (2007) for details.

mation inside relic HII regions might produce stars that typically have masses smaller than the stars that have emitted the radiation. Note that H_2 and HD formation can be further promoted, under certain conditions, in the presence of x-rays or cosmic rays (e.g. Shchekinov & Vasiliev 2004; Kuhlen & Madau 2005; Jasche, Ciardi & Ensslin 2007; Stacy & Bromm 2007). This can be clearly seen in Figure 18, where the evolution of temperature and molecular hydrogen is shown as a function of the density of the gas and of the cosmic rays injection rate.

The reformation mechanism is more efficient than the entropy floor that has been advocated as a mechanism to prevent accretion and cooling of mini-halos in relic HII regions (Oh & Haiman 2003; Kramer, Haiman & Oh 2006). These studies in fact consider adiabatic cooling but, as soon as some H_2 or HD is formed, molecular cooling kicks in and their argument does not apply anymore. In order for it to be valid, gas which is heated but not

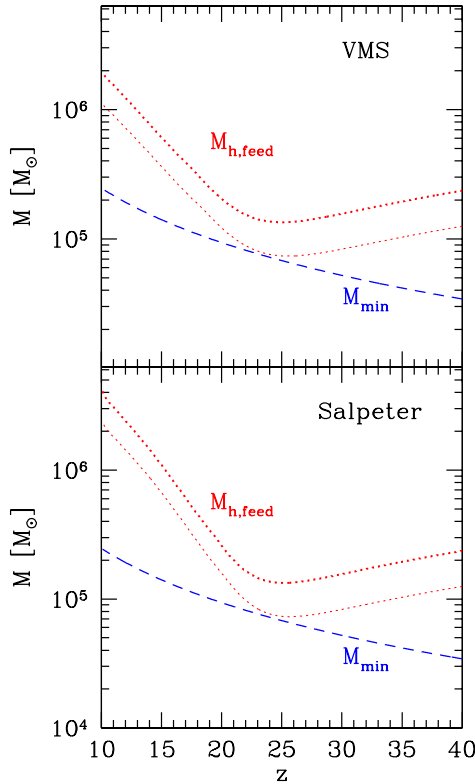


FIGURE 19. Mass evolution with (dotted lines) and without (dashed lines) $\text{Ly}\alpha$ feedback from a population of metal-free stars with a Salpeter IMF (lower panel) or with mass $M_\star = 300 M_\odot$. In objects with mass below $M_{h,feed}$ less than 50% (and as low as 1% for the smallest masses) of the gas is able to collapse compared with a case without feedback. The two dotted lines refer to different models (see Ciardi & Salvaterra 2007 for details).

ionized, e.g. by $\text{Ly}\alpha$ photons (Ciardi & Salvaterra 2007), is needed. An example of this can be seen in Figure 19, where the effect of $\text{Ly}\alpha$ feedback on the ability of the gas to collapse in the presence of a $\text{Ly}\alpha$ background produced by the first, metal-free stars, is shown.

CONCLUSIONS

To conclude, we can summarize feedback effects as follows. In general one can say that:

- feedback strongly depends on the specific local conditions, e.g. metallicity of the gas, density of the gas, intensity of ionizing/dissociating radiation etc etc;
- feedback is not as efficient as naively expected from purely energetic arguments;

- objects with $M > 10^{7-8} M_\odot$ are generally not strongly affected by feedback.

Once a primordial star has formed in a halo:

- star forming regions located in the same halo, but further than a few tens of pc from the star are able to shield against its radiation;
- its UV radiation delays and limit the collapse of cold gas in nearby objects;
- nearby halos generally survive photoevaporation.

After the star dies:

- formation of H_2 and HD in relic HII regions promote structure formation and low-mass, low-metallicity stars might be the outcome.

If the star ends its life as a PISN:

- the host halo is completely disrupted if its mass is $M < 10^6 M_\odot$;
- after the explosion gas in shells can fragment and form small-mass, low metallicity stars;
- metal and dust are expelled and induce a transition to a standard star formation mode.

But several questions still remain at most partially answered, such as: which are the role and characteristics of dust in the early universe? Which is the IMF of the first stars? Which is the efficiency of metal enrichment? Is negative feedback really so negative? Is it possible to have metal-free small-mass stars?

REFERENCES

1. Abel T., Wise J. H., Bryan G. L., 2007, ApJ, 659, L87
2. Ahn K., Shapiro P. R., 2007, MNRAS, 375, 881
3. Alvarez M. A., Bromm V., Shapiro P. R., 2006, ApJ, 639, 621
4. Bromm V., Ferrara A., Coppi P. S., Larson R. B., 2001, MNRAS, 328, 969
5. Bromm V., Loeb A., 2003, Nature, 425, 812
6. Bromm V., Yoshida N., Hernquist L., 2003, ApJ, 596, L153
7. Ciardi B., Bianchi S., Ferrara A., 2002, MNRAS, 331, 463
8. Ciardi B., Ferrara A., Abel T., 2000, ApJ, 533, 594
9. Ciardi B., Ferrara A., Governato F., Jenkins A., 2000, MNRAS, 314, 611
10. Ciardi B., Ferrara A., 2005, Space Science Reviews, 116, 625.
11. Ciardi B., Salvaterra R., 2007, MNRAS, astro-ph/0707.3520
12. Clark P. C., Glover S. C. O., Klessen R. S., 2007, astro-ph/0706.0613
13. Clarke C. J., Oey S., 2002, MNRAS, 337, 1299
14. Dijkstra M., Haiman Z., Rees M. J., Weinberg D. H., 2004, ApJ, 601, 666
15. Dove J. B., Shull J. M., 1994, ApJ, 430, 222
16. Ferrara A., 1998, ApJ, 499, 17L

17. Fujita A., Martin C., Mac Low M.-M., Abel T., 2003, *ApJ*, 599, 50
18. Glover S. C. O., Brand, P. W. J. L., 2001, *MNRAS*, 321, 385
19. Gnedin N. Y., 2000, *ApJ*, 542, 535
20. Greif T. H., Johnson J. L., Bromm V., Klessen R. S., 2007, *astro-ph/0705.3048*
21. Haiman Z., Abel T., Madau P., 2001, *ApJ*, 551, 599
22. Haiman Z., Abel T., Rees M. J., 2000, *ApJ*, 534, 11
23. Haiman Z., Rees M. J., Loeb A., 1997, *ApJ*, 476, 458
bibitem[Heger & Woosley(2002)]HegerWoosley02 Heger
A., Woosley S. E., 2002, *ApJ*, 567, 532
24. Jasche J., Ciardi B., Enßlin T. A., 2007, *astro-ph/0705.4541*
25. Johnson J. L., Bromm V., 2006, 366, 247
26. Johnson J. L., Greif T. H., Bromm V., 2007, *ApJ*, 665, 85
27. Kitayama T., Susa H., Umemura M., Ikeuchi S., 2001, *MNRAS*, 326, 1353
28. Kitayama T., Tajiri T., Umemura M., Susa H. Ikeuchi S., 2000, *MNRAS*, 315, L1
29. Kitayama T., Yoshida N., 2005, *ApJ*, 630, 675
30. Kramer R. H., Haiman Z., Oh S. P., 2006, *ApJ*, 649, 570
31. Kuhlen M., Madau P., 2005, *MNRAS*, 363, 1069
32. Machacek M. M., Bryan G. L., Abel T., 2001, *ApJ*, 548, 509
33. Mackey J., Bromm V., Hernquist L., 2003, *ApJ*, 586, 1
34. Mac Low M.-M., Ferrara A., 1999, *ApJ*, 513, 142
35. Meynet G., Ekström S., Maeder A., 2006, *A&A*, 447, 623
36. Mori M., Ferrara A., Madau P., 2002, *ApJ*, 571, 40
37. Nishi R., Susa H., 1999, *ApJ*, 523, L103
38. Nishi R., Tashiro M., 2000, *ApJ*, 537, 50
39. Oh S. P., Haiman Z., 2003, *MNRAS*, 346, 456
40. Omukai K., Nishi R., 1999, *ApJ*, 518, 64
41. Omukai K., Tsuribe T., Schneider R., Ferrara A., 2005, *ApJ*, 626, 627
42. Oppenheimer B. D., Davé R., 2006, *MNRAS*, 373, 1265
43. O'Shea B., Norman M. L., 2007, *astro-ph/0706.4416*
44. Ricotti M., Gnedin N. Y., Shull J. M., 2002, *ApJ*, 575, 49
45. Ricotti M., Shull J. M., 2000, *ApJ*, 542, 548
46. Salvaterra R., Ferrara A., Schneider R., 2003, *NewA*, 10, 113
47. Santoro F., Shull J. M., 2006, *ApJ*, 643, 26
48. Scannapieco E., Ferrara A., Broadhurst T., 2000, *ApJ*, 536, L11
49. Schneider R., Ferrara A., Natarajan P., Omukai K., 2002, *ApJ*, 571, 30
50. Schneider R., Omukai K., Inoue A. K., Ferrara A., 2006, *MNRAS*, 369, 1437
51. Shapiro P. R., Iliev I. T., Raga A. C., 2004, *MNRAS*, 348, 753
52. Shchekinov Y. A., Vasiliev E. O., 2004, *A&A*, 419, 19
53. Smith B. D., Sigurdsson S., 2007, *astro-ph/07040477*
54. Stacy A., Bromm V., 2007, *astro-ph/0705.3634*
55. Susa H., Kitayama T., 2000, *MNRAS*, 317, 175
56. Susa H., Umemura M., 2004, *ApJ*, 600, 1
57. Susa H., Umemura M., 2006, *ApJ*, 645, 93
58. Tsuribe T., Omukai K., 2006, *ApJ*, 642, L61
59. Vasiliev E. O., Shchekinov Y. A., 2005, *astro-ph/0507603*
60. Wada K., Venkatesan A., 2003, *ApJ*, 591, 38
61. Whalen D., Abel T., Norman M. L., 2004, *ApJ*, 610, 14
62. Wood K., Loeb A., 2000, *ApJ*, 545, 86
63. Yoshida N., Abel T., Hernquist L., Sugiyama N., 2003, *ApJ*, 592, 645
64. Yoshida N., Oh S. P., Kitayama T., Hernquist L., 2007, *ApJ*, 663, 687
65. Yoshii Y., Sabano Y., 1980, *PASJ*, 32, 229